Structural, Electrochemical, and Photophysical Properties of a Molecular Shuttle Attached to an Acid-Terminated Self-Assembled Monolayer

Francesca Cecchet[†] and Petra Rudolf*[,‡]

Laboratoire Interdisciplinaire de Spectroscopie Electronique, Facultés Universitaires Notre-Dame de la Paix, 61 rue de Bruxelles, B-5000 Namur, Belgium, and Materials Science Centre, Rijksuniversiteit Groningen, Nijenborgh 4, NL-9747AG Groningen, The Netherlands

Stefania Rapino, Massimo Margotti, and Francesco Paolucci*

Department of Chemistry "G. Ciamician", University of Bologna, via F. Selmi 2, I-40126 Bologna, Italy

Jacob Baggerman and Albert M. Brouwer*

Institute of Molecular Chemistry, University of Amsterdam, Nieuwe Achtergracht 129, NL-1018 WS Amsterdam, The Netherlands

Euan R. Kay, Jenny K. Y. Wong, and David A. Leigh*

School of Chemistry, University of Edinburgh, West Mains Road, Edinburgh EH9 3JJ, United Kingdom

Received: March 30, 2004; In Final Form: July 6, 2004

A benzylic amide macrocycle containing a pyridine moiety (macrocycle **2**) and a related benzylic amide macrocycle-based molecular shuttle (naphthalimide rotaxane) with two pyridine moieties on the macrocyclic unit were grafted onto a self-assembled monolayer (SAM) of 11-mercaptoundecanoic acid (11-MUA) on gold. X-ray photoelectron spectroscopy (XPS) indicates that the molecules are linked to the SAM by hydrogen-bonding. Electrochemical investigations show that the self-assembled monolayer is densely packed and well ordered and allows the estimation of the average thickness of the SAM alone and of the SAM functionalized with either macrocycle **2** or with naphthalimide rotaxane. The estimated thickness values suggest that the 11-MUA chains in the SAM are tilted with respect to the surface normal, as expected for ordered and stable SAMs, whereas the rotaxane molecules are oriented with the thread parallel to the SAM surface and macrocycle plan preferentially perpendicular to the surface. The photophysical studies of the naphthalimide rotaxane grafted onto the SAM on gold demonstrated that fluorescence is partially quenched but still remains easily measurable because the presence of the SAM reduces the quenching effect of the metal substrate. Moreover, the photophysical analysis clearly indicates that the naphthalimide part of the rotaxane strongly interacts with the carboxylic groups of the SAM, in agreement with the orientation of the molecule obtained from the electrochemistry.

1. Introduction

The design and construction of new architectures for the purpose of developing innovative and promising multifunctional materials is one of the central themes of nanotechnology. Rotaxanes, a class of mechanically interlocked molecules, are proving popular prototypical systems for device applications, because of their unusual structural characteristics. In fact, they are composed of a macrocycle ring locked onto a thread by two bulky stoppers, and the mechanical bond holding together the components of the molecule allows large amplitude relative movements that can be used to modify the molecular properties by external stimuli.[1−4] Various molecular systems in which translational or rotational motion of submolecular components takes place after chemical, electrochemical, electrical or photochemical excitation, have been described previously.[5−14] Up to now, most rotaxane-based submolecular motions have been studied in solution where the large possibility of orientation and ample freedom of movements are allowed. However, the creation of a rotaxane-based device requires the incorporation of rotaxane molecules in bidimensional arrays onto a surface, in a way that preserves the dynamic properties of the molecule. This implies first that the anchoring of the molecules has to ensure that the mutual interactions and the link with the substrate do not affect the molecules' internal degrees of freedom necessary for their use as functional units. Second, the chemical or physical properties of molecules adsorbed on a surface can be slightly or strongly affected and modified, depending on the nature of the substrate and of the adsorbed species, on the distance between the two, and on the presence of an intermediate layer. In addition to these intrinsic difficulties, experimental problems also interfere with the characterization and understanding of the behavior of such surfaces because the number

* Corresponding authors. For thin film preparation and XPS characterization (P.R.): P.Rudolf@phys.rug.nl. For electrochemical measurements (F.P.): francesco.paolucci@unibo.it. For photophysics (A.M.B.): fred@science.uva.nl. For materials (D.A.L.): David.Leigh@ed.ac.uk.

[†] Universitaires Notre-Dame de la Paix.

[‡] Rijksuniversiteit Groningen.

10.1021/jp048621s CCC: $27.50
Published on Web 09/08/2004

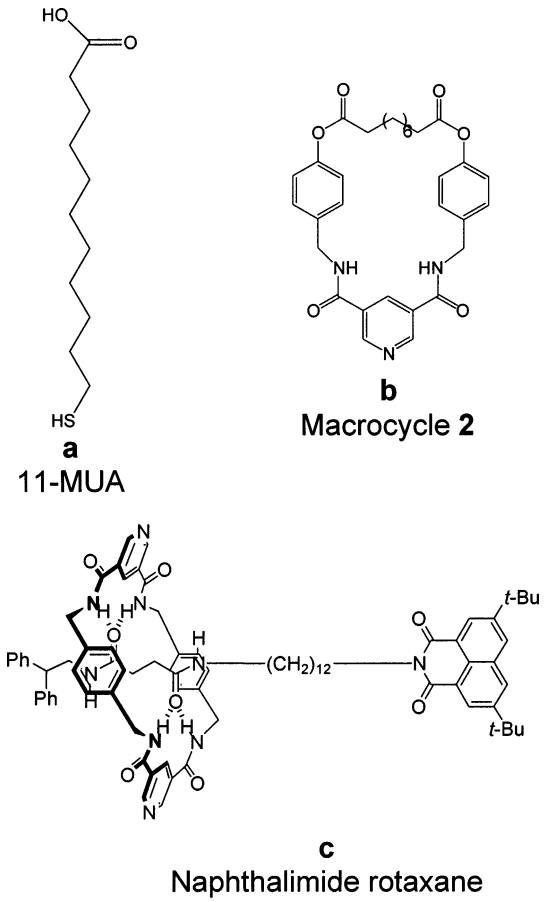

Figure 1. Simplified representation of (a) 11-mercaptoundecanoic acid (11-MUA), (b) macrocycle **2**, and (c) naphthalimide rotaxane.

of molecules adsorbed on the surface is often so low that it falls below the detection limits of many techniques.

A method often used to anchor macromolecular units, such as proteins or enzymes, onto a solid surface is the functionalization of a self-assembled monolayer (SAM) of alkanethiols [see, for example, refs 15−27]. The success of SAMs is due to the simplicity of the experimental procedure to prepare the films, their reproducibility, and the possibility of creating a wide range of surfaces via the incorporation of different groups at the end of the alkyl chains. These groups allow us to graft different types of molecules onto a surface and serve therefore as a starting point from which to build up more complex molecular architectures.

Here a functionalized benzylic amide macrocycle and molecular shuttle were anchored on the surface of an acid-terminated self-assembled monolayer on gold. Macrocycle **2** (Figure 1b) contains a pyridine function that allows grafting by hydrogen bonding with the acid groups of SAM, as already shown in a previous work.[28] Similarly, the naphthalimide rotaxane molecule (Figure 1c) contains two pyridine moieties localized on the macrocycle unit and is hence also expected to hydrogen-bond to the SAM. A similar rotaxane with two phenyl groups in the place of the two pyridine groups on the macrocycle already demonstrated behavior as a molecular shuttle in solution, either after excitation by a laser pulse[10] or after electron transfer at an electrode.[11]

The aim of this work has been to investigate the structural, electrical, and/or the photophysical properties of such surfaces, focusing the attention especially on the packing, the order, and the thickness of macrocycle and rotaxane films, and on the photoluminescent properties of the naphthalimide rotaxane films on gold.

2. Experimental Section

Materials. Macrocycle **2** and naphthalimide rotaxane (Figure 1b,c) were synthesized using methods analogous to those previously described in the literature.[29] 11-Mercaptoundecanoic acid (95%, Aldrich) (Figure 1a), chloroform, and dichloromethane (HPLC grade, Acros) were used as supplied.

Preparation of Monolayers. The substrates were evaporated gold films supported on Si(111) wafers (IMEC, Belgium). They were cleaned in an ozone discharge for 15 min, followed by sonication in ethanol for 20 min immediately before being employed. Carboxylic acid-terminated SAMs were prepared by immersion of the gold substrates in a 1 mM chloroform solution of 11-MUA for 21 h. The samples were rinsed in chloroform and dried under argon before contact angle measurements or introduction into ultrahigh vacuum for characterization by X-ray photoelectron spectroscopy (XPS).

Functionalization Using Macrocycle 2. Grafting of macrocycle **2** onto the SAM surface has been carried out after 98 h of immersion of the 11-MUA monolayer in a 1 mM solution of macrocycle **2** in dichloromethane, as described in the literature.[28]

Functionalization Using Naphthalimide Rotaxane. For grafting the rotaxane molecules, the carboxylic acid-terminated SAMs were immersed in a 0.1 mM solution of naphthalimide rotaxane in dichloromethane for 120 h.

The modified surfaces were each rinsed and sonicated for 30 s in pure dichloromethane and dried under a stream of argon and then characterized by XPS, cyclic voltammetry, impedance spectroscopy, and fluorescence spectroscopy.

X-ray Photoelectron Spectroscopy (XPS) Analysis. XPS measurements were performed using a SSX-100 (Surface Science Instruments) photoelectron spectrometer with a monochromatic Al Kα X-ray source ($h\nu = 1486.6$ eV). The energy resolution was set to 0.92 eV to minimize data acquisition time and the photoelectron takeoff angle (TOA) was 90°. All binding energies were referenced to the Au $4f_{7/2}$ core level.[30] The base pressure in the spectrometer was in the low 10^{-10} Torr range.

Spectral analysis included a linear background subtraction and peak separation using mixed Gaussian−Lorentzian functions, in least squares curve-fitting program (Winspec) developed in the LISE laboratory of the Facultés Universitaires Notre-Dame de la Paix, Namur, Belgium. The photoemission peak areas of each element, used to estimate the amount of each species on the surface, were normalized by the sensitivity factors of each element tabulated for the spectrometer used.

Electrochemical Instrumentation and Measurements. The electrochemical experiments were performed in unbuffered 0.1 M KCl aqueous solutions using a two-compartment electrochemical cell fitted with a saturated calomel electrode (SCE) and a platinum spiral as counter electrode. Cyclic voltammetry (CV) and electrochemical impedance spectroscopy (EIS) experiments were carried out with an Autolab Model PGSTAT 30.

Fluorescence Spectroscopy. Steady-state spectra of the films were recorded on a Spex Fluorolog 3 spectrometer, equipped with two double grating monochromators in the excitation and emission channels. A front-face geometry was used, with an angle of 20° between excitation and detection directions. The detector was a Peltier cooled R636-10 (Hamamatsu) photomultiplier tube.

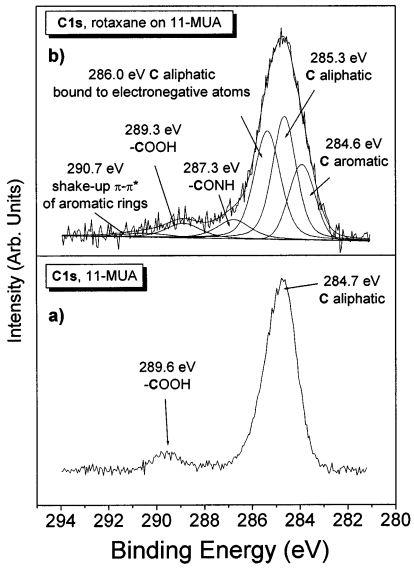

Figure 2. Photoemission spectra and fit of the C 1s core level region for (a) a film of 11-MUA and (b) a film of 11-MUA functionalized with naphthalimide rotaxane.

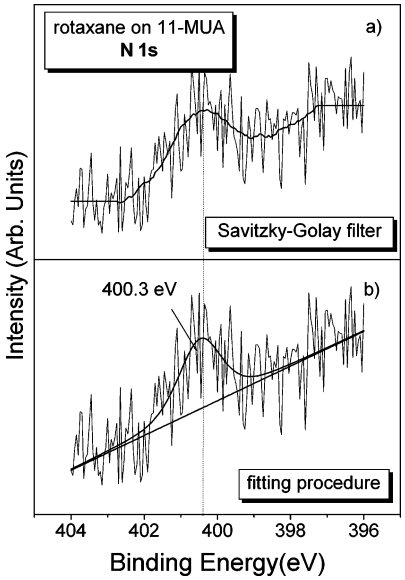

Figure 3. Photoemission spectra of the N 1s core level region for a film of 11-MUA functionalized with naphthalimide rotaxane: (a) experimental curve and fit; (b) experimental curve and Savitzky−Golay filtered curve.

Time-resolved fluorescence measurements were performed using a Hamamatsu streak camera system, consisting of a Chromex IS250 spectrograph, a M5677 slow-speed sweep unit, a C4792 trigger unit, a C5680 blanking unit, and a C4742-95 digital CCD camera.[31] The sample was excited using an LTB MSG400 nitrogen laser (337 nm, fwhm $\approx$ 0.9 ns, 10 Hz). Excitation and emission light were guided via optical fibers in a front-face geometry. For analysis the data were imported into the Igor Pro 4.0 data analysis package (Wavemetrics, Inc., Lake Oswega, OR). The system response (scattered laser light) was modeled as a Gaussian function, and the decay traces were fitted to the convolution of a Gaussian pulse and an exponential decay.

3. Results and Discussion

XPS Analysis. Figure 2, bottom panel, shows the carbon 1s core level photoemission spectrum for a monolayer of 11-MUA. As already discussed in a previous work for films of macrocycle **2**,[28] to analyze these data, we mathematically reconstruct the spectrum with a minimum number of peaks consistent with the raw data and the molecular structure of the film, with the simplification of assuming equivalent carbon atoms for chemical environments that are expected to give very close values of the binding energy. Following this procedure, the analysis of the carbon 1s core level region recorded for the monolayer provides the identification of three contributions to the experimental curve: a first main peak, at 284.7 eV, is assigned to the aliphatic carbons of the alkyl chains. The main peak is slightly asymmetric due to the contribution at higher binding energy (0.3−0.5 eV from the pure aliphatic carbons) of the carbon atom bound to the acid group and to a possible CO atmospheric contamination. The last peak at 289.6 eV corresponds to the carboxylic carbon.[28−35] The analysis of the carbon 1s core level region for a SAM of 11-MUA represents the starting point to characterize the functionalization process with macrocycle **2**[28] or with naphthalimide rotaxane.

Figure 2, top panel, shows the C 1s core level region for a monolayer functionalized with naphthalimide rotaxane molecules: as can be clearly seen, there are several differences between the spectrum recorded for the SAM alone and for the SAM modified with the rotaxane, confirming that they refer to different situations. If we compare these two spectra and rely on the characteristic peak energies for the different carbon species reported in the literature,[35−37] we can assign all fitted peaks to chemical species present in the SAM functionalized with rotaxane molecules. The peak at 284.6 eV is the signature of aromatic carbons, which occur only in the rotaxane. The peak at 285.3 eV can be assigned either to aliphatic carbon atoms or to aromatic carbons bound to electronegative groups. The peak at 286.0 eV corresponds to aliphatic carbons of the rotaxane bound to electronegative atoms such as N or O. At 287.3 eV binding energy we see the peak characteristic of amide and imide carbons of the rotaxane, and at 289.3 eV the contribution of carboxylate carbons. The shake-up feature associated with the aromatic rings of the rotaxane is found at 290.7 eV.

Figure 3 bottom panel shows the N 1s core level spectrum recorded for the SAM functionalized with naphthalimide rotaxane. The presence of a signal in this region is the most convincing evidence that rotaxane is grafted on the surface of the self-assembled monolayer because nitrogen occurs only in the rotaxane. The experimental curve is very weak and noisy because nitrogen has a small photoionization cross-section and because the molecule contains only 9 nitrogen atoms whereas the other 88 atoms are other elements (H is here not computed). However, the fitting procedure allowed us to evidence a single peak at 400.3 eV binding energy corresponding to the amide, imide, and pyridine nitrogen atoms of the naphthalimide rotaxane. To validate the peak assignment obtained from the fitting procedure, we treated the same experimental curve with a Savitzky−Golay filter method,[38] which has the peculiarity of preserving features of the data such as peak height and width. The result is shown in Figure 3, top panel: the experimental curve smoothed with this method shows a peak centered at 400.3 eV, i.e., at exactly the same energy as the peak obtained from the fitting procedure. As shown previously[28] for macrocycle **2** films, the fact that the nitrogen 1s experimental curve is fitted with a single peak gives information on the interaction between the macrocycle and SAM. In general, one expects the signature of the pyridine nitrogen at a binding energy between 399.0 and 399.5 eV depending on the chemical environment of the pyridine rings.[35] However, theoretical calculations investigating the

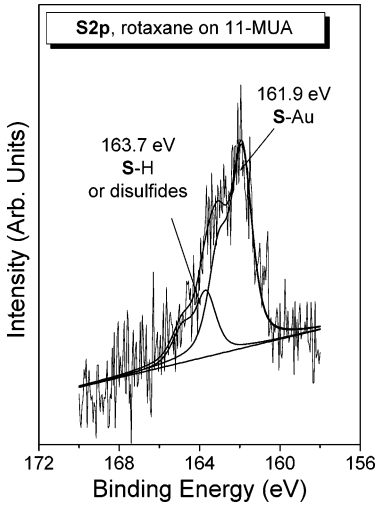

Figure 4. Photoemission spectrum and fit of the S 2p core level region for a film of 11-MUA functionalized with naphthalimide rotaxane.

effects of intra- and intermolecular interactions on the binding energy for similar molecules, i.e., benzylic amide catenanes, showed that hydrogen bonding interactions can produce shifts to a higher binding energy of up to 1 eV.[39] In addition, shifts up to 1.7 eV have been already observed for pyridine moieties interacting with acid groups by hydrogen bonding.[40] However, an electrostatic interaction between a protonated pyridine nitrogen and an anionic carboxylate function following the exchange of the proton of the carboxylic acid group, should give rise to a new component in the N 1s core level region between 401.0 and 402.0 eV.[35] The N1s signal is quite weak, and therefore we cannot easily identify a possible second contribution at higher binding energy, between 401 and 402 eV; however, the raw data indicate that such a contribution, if it exists, has to be sensibly weaker than the main component at 400.3 eV. We can therefore conclude that the majority of the rotaxane molecules links to the SAM by a hydrogen-bonding interaction between the pyridine nitrogen localized on the macrocycle unit of the naphthalimide rotaxane and the acid group of SAM, similarly to what was already evidenced for the macrocycle **2** alone grafted onto SAM.[28]

Figure 4 shows the S 2p core level region for the SAM functionalized with the naphthalimide rotaxane: the fitting of the experimental curve clearly shows two contributions, one where the S $2p_{3/2}$ is found at 161.9 eV and which is assigned to sulfur bonded to gold,[30,41] and the other component with the S $2p_{3/2}$ peak at 163.7 eV which could be due to a small amount of alkanethiols not covalently bonded to the substrate but only intercalated between 11-MUA molecules bound to Au or physisorbed as a double layer.[30,41] Alternatively, the second component might derive from disulfides formed under the influence of the X-rays during spectral acquisition.[42−44] No oxidized species of sulfur can be detected at binding energies of 164.8 and 168.5 eV.[45]

Quantitative analysis of XPS spectra allows us to determine the yield of functionalization of the SAM with naphthalimide rotaxane molecules: from the photoemission peak area of each element the amount of that species on the surface is obtained. We compared the experimentally determined atomic percentages with atomic ratios calculated for different functionalization yields of the acid groups of the SAM: in the calculation we considered a model surface of 100 thiol chains and computed the atomic percentages for C, O, S, and N (excluding hydrogen which cannot be detected by XPS) for coverages of 1, 3, 5, 10, 20, and up to 100 rotaxane molecules. The error on the photoemission peak areas was estimated depending on the signal/noise ratio in the spectrum for each element: the carbon and oxygen signals are better defined; hence the error was found to be 2% and 5%, respectively. Sulfur and nitrogen signals are weaker, producing noisier spectra, and therefore more substantial errors in the peak areas, estimated at 10% and 15%, respectively. Table 1 shows the experimental values obtained from our film and the theoretical ones computed for functionalization of 1%, 3%, 5%, and 10% of the acid groups. C and especially the O signal always contain a contribution of atmospheric contaminants, which affect all percentages. Namely, the percentages of C and O increase and consequently the percentages of S and N decrease. However, the N/S ratio, which is not affected by contaminants, and the comparison between theoretical and experimental data clearly indicate that the functionalization of the SAM by the rotaxane molecules is close to 3%, whereas the theoretical data assuming that 1%, 5%, or 10% of the acid groups are functionalized with rotaxane molecules strongly deviate from the experimental data.

TABLE 1: Comparison between Experimental Atomic Percentages Derived from the Photoemission Peak Areas of 11-MUA Film Functionalized with Naphthalimide Rotaxane and Theoretical Values Calculated for Different Coverages[a]

	exptl atomic percentages	th 1%	th 3%	th 5%	th 10%
% C	78.1 ± 1.6	78.9	79.3	79.7	80.3
% O	16.1 ± 0.8	13.9	13.2	12.7	11.7
% S	4.5 ± 0.5	6.7	5.9	5.3	4.2
% N	1.2 ± 0.2	0.6	1.6	2.4	3.8
N/S	0.27 ± 0.05	0.09	0.27	0.45	0.90

[a] The error on the experimental atomic percentages was estimated to be 2% for C, 5% for O, 10% for S, and 15% for N.

Electrochemistry. The electrochemical properties of 11-MUA SAMs, both pristine and functionalized with macrocycle **2** or with naphthalimide rotaxane, were investigated by cyclic voltammetry (CV) and electrochemical impedance spectroscopy (EIS). Both techniques have been widely used, in either the presence or the absence of a redox probe, on one hand to determine the size and number of defects in the SAM, and on the other to evaluate the double layer capacitance of the modified electrode and whence the average thickness of the organic layer.[46,47] Though in CV large potential sweeps (of the order of 0.1 to 1 V) are applied to the electrode/solution interface and the resulting dc current is measured, in EIS the interface is usually kept at its rest potential and probed by using a small-amplitude (typically $\leq$20 mV) sinusoidal voltage. Hence EIS is a much less disturbing technique than CV.[48,49] Excitation frequencies (f) ranging between 1 mHz and 1 MHz can be used, permitting the investigation of phenomena with time scales ranging over 9 decades, which may be resolved in principle according to their relaxation time.

Both CV and EIS confirmed the very low level of defects present in the 11-MUA monolayer. In particular, Figure 5 shows the CV curves relative to $[Fe(CN)_6]^{3-/4-}$ reduction/oxidation obtained at the unmodified gold electrode (dotted line) and at the gold electrode modified with 11-MUA (solid line). No microelectrode-type behavior, typical of the presence of pinholes in the film,[46] was observed in the CV curve associated with the 11-MUA modified gold surface, indicating that electron transfer occurs preferentially by through-film tunneling.[46,50−52] The very low level of defects in the film was also assessed by performing an EIS analysis under the conditions of Figure 6. [The presence of unbound or disulfide thiol species evidenced by XPS could introduce defect sites in the monolayer; however, the latter did not affect the electrochemical blocking behavior of the SAM,

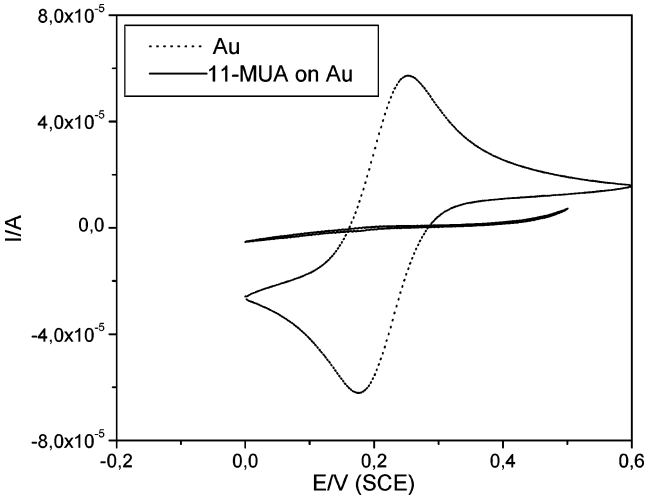

Figure 5. Cyclic voltammetry curves recorded for pure gold electrode (···) and for a SAM of 11-MUA (—) in a 0.1 M KCl aqueous solution, at 50 mV/s.

as evidenced by our electrochemical experiments.] In this figure the out-of-phase component of the impedance, Z'', is plotted vs the in-phase one, Z' where Z'' and Z' are the parametric functions of the frequency (Z plot or Nyquist plot).[47,48] Figure 6a shows the impedance spectra obtained at various potentials: the incomplete semicircles that rapidly shrink upon increasing overpotential (under the present conditions, the open circuit potential, E_{oc}, coincides with $E°_{[Fe(CN_6)]^{3-/4-}} = 0.18$ V) are associated with the slow electron transfer kinetics experienced by the redox probe at the modified electrode.[46−48] An alternative presentation of the impedance data is shown in Figure 6b where the complex capacitance C is displayed (C plot). C is defined as $1/j\omega Z$, where $j = -1^{1/2}$ and ω is the angular frequency ($=2\pi f$). The C plot emphasizes the interface response at higher frequencies with respect to the Z plot.[53,54] Notice that, in the framework of an equivalent circuit description of the electrochemical interface,[47,48] a semicircle in the Z plot corresponds to a parallel RC (resistor, capacitor) arrangement and a straight vertical line to a series RC arrangement, and vice versa in the case of C plot. The prominently blocking behavior of the 11-MUA monolayer is evidenced by the semicircle observed in the C plots in the medium-to-high frequency range, both in the presence of the redox couple and in its absence. A second (incomplete) semicircle occurring at relatively lower frequencies, is associated with a parallel charging path characterized by a higher time constant (likely associated with protonation/deprotonation and/or diffusion processes, vide infra), whereas only in the low-frequency range do slow processes associated with charge transfer involving $[Fe(CN)_6]^{3-/4-}$ or diffusion take place (compare, in Figure 6b, the two plots obtained in the presence and in the absence of the redox probe). The electrical response of the interface was described in terms of the equivalent circuit shown in Figure 6. R_Ω represents the solution resistance, C_{dl} the double layer capacitance, and R_{ct} the charge transfer resistance (related to the exchange current i_0[49] and clearly omitted in the case of data obtained in the absence of redox couple). The electrical parameters were evaluated by fitting procedures, using the CNLS method described by Boukamp.[55] In analogy with other equivalent circuits proposed for describing the electrical behavior of a thick SAM,[56] the branch comprising the element R_{SAM}, C_{SAM}, and the Warburg element Z_w, were introduced to reproduce the behavior at $f < 1$ Hz. Such elements are associated with physical processes occurring at the interface such as desorption/adsorption of protons at the terminal acid groups[46] and/or diffusion within the SAM at grain boundaries or other defects in the film.[53,57] The best-fit values of the various elements in the circuit of Figure 6, measured at the E_{oc}, are reported in Table 2. From the value of R_{ct} obtained at E_{oc} ($=E°$),

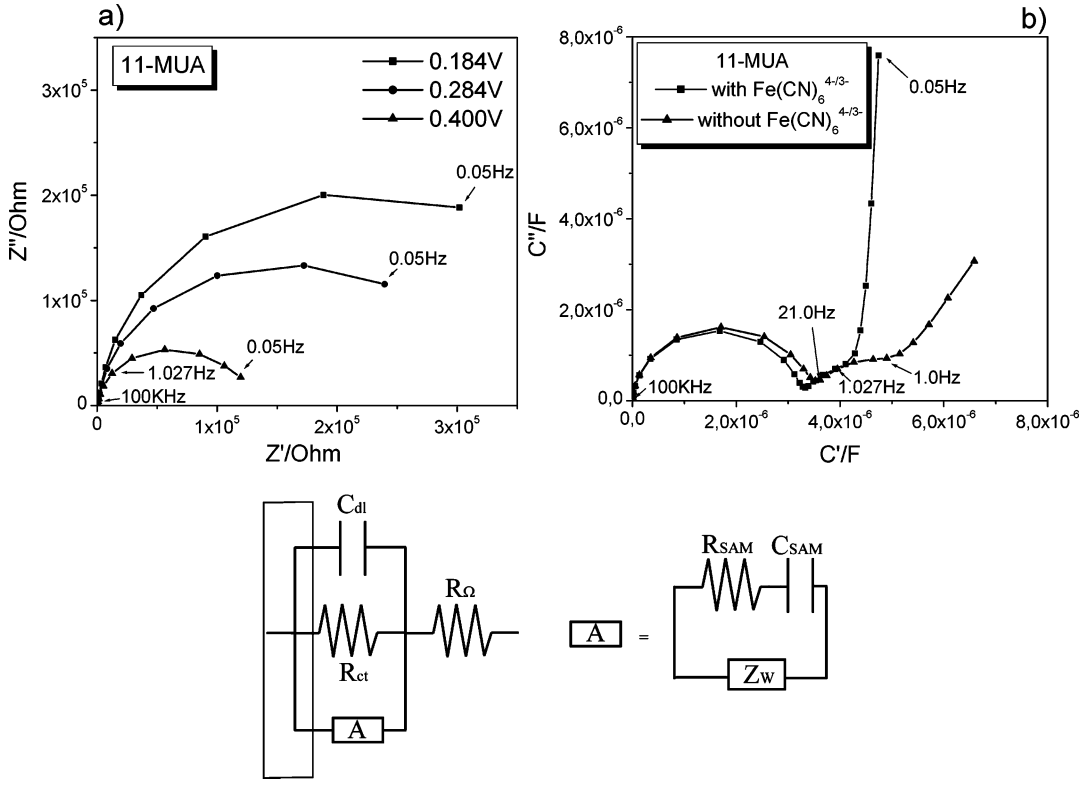

Figure 6. (a) Nyquist plots recorded for a film of 11-MUA in a 0.1 M KCl aqueous solution 1 mM of $Fe(CN)_6^{3-/4-}$: 0.1 M of KCl at 0.184 V (■), at 0.284 (●), and at 0.400 V (◆). (b) C plots recorded for a film of 11-MUA in a 0.1 M KCl aqueous solution (▲) and 1 mM of $Fe(CN)_6^{3-/4-}$ (■). (c) Representation of the equivalent circuit associated with the electrochemical interface solution/SAM/gold.

TABLE 2: Electrical Parameters Associated with the Solution/SAM/Gold Electrochemical Interface Obtained from Fitting of EIS Spectra of Figure 6 by Using the Equivalent Circuit Shown in Schematic Form in the Lower Part of Figure 6

potential, V	R_Ω, Ω	R_{SAM}, kΩ	R_{ct}, kΩ	C_{dl}, μF cm^{-2}	C_{SAM}, μF cm^{-2}	$10^{-6}W$
0.184	55.1	0.485	60.6	3.19	0.752	0.798
0.284	55.1	0.339	35.4	3.05	0.787	1.270
0.400	55.1	0.133	19.1	3.00	0.867	7.705

the standard heterogeneous constant, k^0, was estimated using the equation[48,49]

$$k^0 = (RT/n^2F^2AC_0)(1/R_{ct}) \quad (1)$$

and found to be equal to 1.1×10^{-6} cm s^{-1}. On the other hand, the value for k^0 at the clean gold surface is 0.031 cm s^{-1},[58] whence, according to the relationship for tunneling

$$k_{SAM} = k_{Au}e^{-(\beta d)} \quad (2)$$

an electronic tunneling factor $\beta = 0.93/CH_2$ was obtained. This is in very good agreement with reported values of β for alkanethiols[50,51,59] and confirms the highly blocking nature of the 11-MUA monolayer. Furthermore, the low value of C_{dl} (Table 2) is also typical of electrodes covered by a well-formed SAM of long-chain thiols.[46] Within the Helmholtz capacitor approximation of the double layer and assuming a dielectric constant of the organic layer $\epsilon = 4 \pm 1$,[46] we find from the best-fit value for C_{dl} that the average thickness of the SAM amounts to $t = \epsilon\epsilon_0/C_{dl} = 12.5 \pm 0.6$ Å^2. Taking into account the length of the 11-MUA molecule (16.1 Å), this value for t indicates that 11-MUA forms a close-packed SAM with molecules tilted between 35° and 40° from the surface normal.

[To validate the SAM thickness value obtained by capacitance measurements, we calculated the average thickness by XPS: following the procedure outlined by Whelan et al. (*Appl. Surf. Sci.* **1998**, *134*, 144), we calculated the layer thickness for the SAM from the data collected on the Au substrate before and after immersion in the alkanethiol solution, and we found a thickness value of ~10 Å. This value is comparable but slightly lower than the one obtained by electrochemistry because the gold surface was analyzed by XPS before immersion in the alkanethiol solution and therefore the "clean" Au 4f signal is necessarily attenuated by the hydrocarbon contaminants from the environment, leading to an underestimation of the Au 4f signal attenuation by the SAM.]

Functionalization of the 11-MUA monolayer with macrocycle **2** leads to a sizable modification of its electrochemical properties. Figure 7a compares the complex capacitance spectra of the 11-MUA functionalized with macrocycle **2** with that of the pristine 11-MUA monolayer. A very similar behavior is observed at both high and low frequencies. However, the smaller semicircle observed for the macrocycle **2** covered SAM, and hence the lower value of C_{dl} (2.1 μF cm^{-2}), suggest that the functionalization does not alter significantly the compactness of the SAM and that macrocycle molecules form an additional, and still relatively densely packed, insulating layer on top of the 11-MUA monolayer. By assuming in first approximation that the same relative permittivity pertaining to the 11-MUA monolayer may be used also for the SAM functionalized with macrocycle **2**, an increased Helmholtz capacitor thickness of 16.9 ± 0.9 Å is obtained.

Analogous results were obtained in the case of 11-MUA functionalized with naphthalimide rotaxane, as shown in Figure 7b, where the *C* plot relative to the pristine 11-MUA monolayer is compared to the *C* plot relative to 11-MUA functionalization with naphthalimide rotaxane. Apparently, only the capacitive properties of the film are affected by functionalization because the EIS spectra display the same high-frequency semicircle, but with a significant decrease of diameter. The corresponding C_{dl} value (2.4 μF cm^{-2}) is very close to that measured for the macrocycle **2** film: this suggests the rotaxane molecules are arranged with the thread parallel to the surface, in agreement with a grafting process in which the pyridine moieties, localized on the macrocycle are hydrogen-bound to the acid groups. In fact, if one considers the size of the naphthalimide molecular shuttle (the linear thread's length is about 35 Å and the macrocycle's diameter ~10 Å), the average thickness estimated by capacitance measurements is justified only on the basis of an orientation of the molecule with the thread parallel to the 11-MUA surface and the macrocycle plan perpendicular to it. Moreover, the orientation of the rotaxane molecules gives an explanation of the low functionalization yield estimated by XPS: by relating the size of a naphthalimide rotaxane molecule to the distance between two sulfur atoms (which is about 5 Å),[60] one concludes that 3% of functionalization represents a quite high level of coverage of the self-assembled monolayer surface.

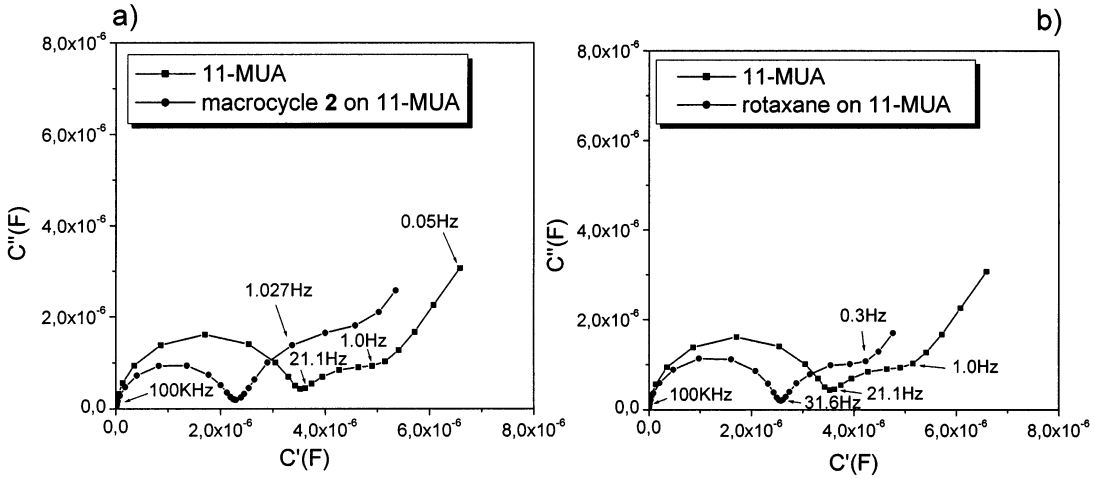

Figure 7. (a) *C* plots recorded for a SAM of 11-MUA (■) and for a SAM of 11-MUA functionalized with macrocycle **2** (●) in a 0.1 M KCl aqueous solution and (b) *C* plots recorded for a SAM of 11-MUA (■) and for a SAM of 11-MUA functionalized with rotaxane (●) in a 0.1 M KCl aqueous solution.

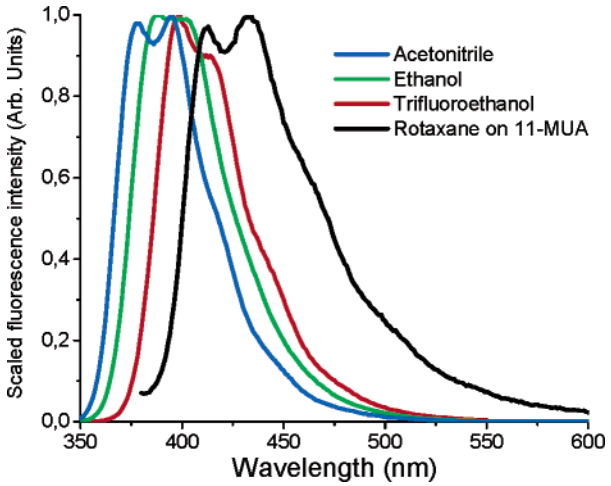

Figure 8. Fluorescence emission spectra of the rotaxane in acetonitrile (blue line), ethanol (green line), and trifluoroethanol (red line), and on 11-MUA (black line).

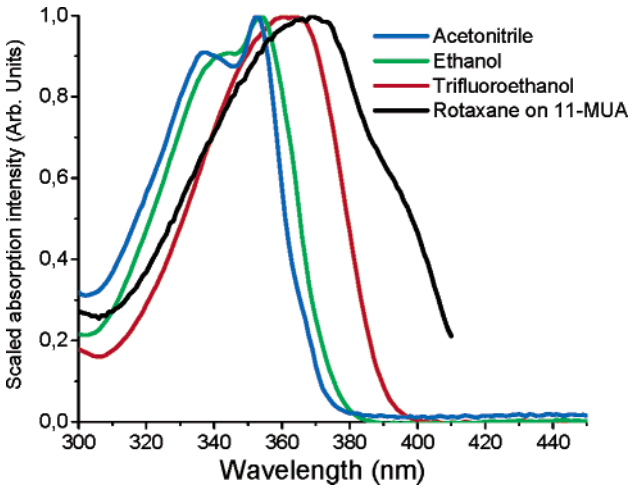

Figure 9. Absorption spectra of the rotaxane in acetonitrile (blue line), ethanol (green line), and trifluoroethanol (red line) and fluorescence excitation spectrum ($\lambda_{em} = 435$ nm) of the rotaxane on 11-MUA (black line).

Fluorescence Spectroscopy. The fluorescence emission spectra of the naphthalimide rotaxane on the SAM are shown in Figure 8 together with the spectra measured in acetonitrile, ethanol, and trifluoroethanol solutions. The fluorescence decay times in these solvents are 1.6, 2.3, and 3.3 ns, respectively. Unfortunately, the signal from the rotaxane on the SAM was too weak to permit a reliable lifetime measurement. The excitation spectrum of the naphthalimide rotaxane on the SAM is shown in Figure 9, together with the absorption spectra in solution. Both the excitation and the emission spectrum, which are due to the naphthalene imide chromophore, are substantially shifted to lower energy compared to the spectra in solution. The similar shapes of the emission spectra can be taken as an indication that the emissive species are not essentially different; i.e., strong intermolecular associations between the chromophores on the SAM can be ruled out.[61] The red shift of the spectra is likely to be due to hydrogen bonding between the imide carbonyl groups and the carboxylic acids in the SAM. It is known for naphthalimides that the fluorescence red shifts with increasing polarity and proticity of the solvent.[62] The systematic red shift of the bands in the series acetonitrile−ethanol−trifluoroethanol correlates with an increase in the hydrogen bond donating capacity of the solvents. In solution, the red shift is accompanied by a substantial increase of the excited-state lifetime.

The fluorescence results demonstrate that not only the pyridine rings, but also the naphthalimide part of the rotaxane is strongly interacting with the carboxylic groups of the SAM, confirming that the thread is oriented parallel to the surface. Strong interchromophore interaction is not apparent. Although the fluorescence of the naphthalimide rotaxane molecules is partially quenched by the nearby gold surface, it is still easily measurable. This implies that it should be possible to detect a shuttling process, induced by some external stimulus, by means of fluorescence spectroscopy. Design and synthesis of molecular systems in which this concept can be realized are in progress.

4. Conclusions

A benzylic amide macrocycle and rotaxane have been physisorbed onto an acid-terminated self-assembled monolayer on gold. XPS characterization suggests that the molecules are held in place by hydrogen-bonding between the pyridine moieties of the macrocycle and the acid functions of SAM. Electrochemical investigations indicate a well-packed and ordered self-assembled monolayer with a very low fraction of defects, giving reason to the adsorption of macrocycle and naphthalimide rotaxane molecules on top of SAM and not intercalated between the thiol chains. Moreover, by capacitance measurements it was possible to estimate the averaged thickness of SAM and SAM functionalized with macrocycle or rotaxane: the thickness found for SAM is in agreement with the molecular length of 11-MUA thiol assuming a tilting angle of 35−40° from the normal to the surface, as expected for the ordered and stable structure of SAM. The increase in film thickness for macrocycle **2** on SAM and naphthalimide rotaxane on SAM indirectly confirms the functionalization process. In addition, from the film thickness and from dimensional considerations the orientation of rotaxane molecules onto the SAM surface was inferred, with the thread parallel to the surface and the macrocycle plan preferentially perpendicular to the surface in the conformation useful for the interaction of one pyridine moiety with an acid group. The fluorescence properties of naphthalimide rotaxane adsorbed on the acid-terminated SAM on gold showed that fluorescence is partially quenched due to the gold substrate; however, it is still easily measurable because of the presence of the intermediate SAM reduces the quenching effect. Moreover, the photophysical analysis clearly indicated that also the naphthalimide part of the rotaxane is strongly interacting with the carboxylic groups of the SAM, which validates the orientation of the molecules with the thread parallel to the surface, as inferred from electrochemistry.

Acknowledgment. This work was performed within the EU RT network EMMMA contract no. HPRN-CT-2002-00168 and received additional support from the EU contract MECHMOL no. IST-2001-35504, from PAI P5/01, from MIUR the University of Bologna, from FOM (Netherlands) and from the Breedtestrategie program of the Rijksuniversiteit Groningen. This research was also supported in part by The Netherlands Organization for the Advancement of Research (NWO).

References and Notes

(1) Johnston, A. G.; Leigh, D. A.; Nezhat, L.; Smart, J. P.; Deegan, M. D. *Angew. Chem., Int. Ed. Engl.* **1995**, *34*, 1212.

(2) Leigh, D. A.; Moody, K.; Smart, J. P.; Watson, K. J.; Slawin, A. M. Z. *Angew. Chem., Int. Ed. Engl.* **1996**, *35*, 306.

(3) Leigh, D. A.; Murphy, A.; Smart, J. P.; Slawin, A. M. Z. *Angew. Chem., Int. Ed. Engl.* **1997**, *36*, 728.

(4) Johnston, A. G.; Leigh, D. A.; Murphy, A.; Smart, J. P.; Deegan, M. D. *J. Am. Chem. Soc.* **1996**, *118*, 10662.
(5) Dietrich-Buchcker, C.; Sauvage, J.-P. *Bioorg. Chem. Frontiers* **1991**, *2*, 195.
(6) Bissell, R. A.; Cordova, E.; Kaifer, A. E.; Stoddart, J. F. *Nature* **1994**, *369*, 133.
(7) Kelly, T. R.; Sestelo, J. P.; Telliu, I. *J. Org. Chem.* **1998**, *63*, 3655.
(8) Collier, C. P.; Wong, E. W. Belohradsky, M.; Raymo, F. M. Stoddart, J. F.; Kuekes, P. J.; Williams, R. S.; Heath, J. R. *Science* **1999**, *285*, 391.
(9) Bermudez, V.; Capron, N.; Gase, T.; Gatti, F. G.; Kazjar, F.; Leigh, D. A.; Zerbetto, F.; Zhang, S. *Nature* **2000**, *406*, 608.
(10) Brouwer, A. M.; Frochot, C.; Gatti, F. G.; Leigh, D. A.; Mottier, L.; Paolucci, F.; Roffia, S.; Wurpel, G. W. H. *Science* **2001**, *16*, 2124.
(11) Altieri, A.; Gatti, F. G.; Kay, E. R.; Leigh, D. A.; Paolucci, F.; Slawin, A. M. Z.; Wong, J. K. Y. *J. Am. Chem. Soc* **2003**, *125*, 8644.
(12) Cavallini, M.; Biscarini, F.; León, S.; Zerbetto, F.; Bottari, G.; Leigh, D. A. *Science* **2003**, *299*, 531.
(13) Leigh, D. A.; Wong, J. K. Y.; Dehez, F.; Zerbetto, F. *Nature* **2003**, *424*, 174−179.
(14) Bottari, G.; Leigh, D. A.; Pérez, E. M. *J. Am. Chem. Soc.* **2003**, *125*, 13360−13361.
(15) Azehara, H.; Mizutani, W.; Suzuki, Y.; Ishida, T.; Nagawa, Y.; Tokumoto, H.; Hiratani, K. *Langmuir* **2003**, *19*, 2115.
(16) Ferretti, S.; Paynter, S.; Russell, D. A.; Sapsford, K. E.; Richardson, D. J. *Trends Anal. Chem.* **2000**, *9*, 19.
(17) Allara, D. *Biosensor Bioelectron.* **1995**, *10*, 771.
(18) Higashi, N.; Takahashi, M.; Niwa, M. *Langmuir* **1999**, *15*, 111.
(19) Madoz, J.; Kuznztzov, B. A.; Medrano, F. J.; Garcia, J. L.; Fernandez, V. M. *J. Am. Chem. Soc.* **1997**, *119*, 1043.
(20) Blonder, R.; Willner, I.; Buckmann, F. *J. Am. Chem. Soc.* **1998**, *120*, 9335.
(21) Jordan, C. E.; Frey, B. L.; Kornguth, S.; Corn, R. M. *Langmuir* **1994**, *10*, 3642.
(22) Ostuni, E.; Yan, L.; Whitesides, G. M. *Colloids Surf. B: Biointerfaces* **1999**, *15*, 3.
(23) Gooding, J. J.; Hibbert, D. B. *Trends Anal. Chem.* **1999**, *8*, 18.
(24) Patel, N.; Davies, M. C.; Hartshorne, M.; Heaton, R. J.; Roberts, C. J.; Tendler, S. J. B.; Williams, P. M. *Langmuir* **1997**, *13*, 6485.
(25) Jiang, L.; Glidle, A.; Griffith, A.; McNeil, C. J.; Cooper, J. M. *Bioelectrochem. Bioenerg.* **1997**, *42*, 15.
(26) Yang, H. C.; Dermody, D. L.; Xu, C.; Ricco, A. J.; Crooks, R. M. *Langmuir* **1996**, *12*, 726.
(27) Strither, T.; Cai, W.; Zhao, X.; Hamers, R. J.; Smith, L. M. *J. Am. Chem. Soc.* **2000**, *122*, 1205.
(28) Cecchet, F.; Pilling, M.; Hevesi, L.; Schergna, S.; Wong, J. K. Y.; Clarkson, G. J.; Leigh, D. A.; Rudolf, P. *J. Phys. Chem. B* **2003**, *107*, 10863.
(29) Lane, A. S.; Leigh, D. A.; Murphy, A. *J. Am. Chem. Soc.* **1997**, *119*, 11092.
(30) Moulder, J. F.; Stickle, W. F.; Sobol, P. E.; Bomben, K. D. *Handbook of Photoelectron Spectroscopy*; Perkin-Elmer Corporation, Physical Electronics Division: Eden Prairie, MN, 1992.
(31) Lauteslager, X. Y.; van Stokkum, I. H. M.; van Ramesdonk, H. J.; Brouwer, A. M.; Verhoeven, J. W. *J. Phys. Chem. A* **1999**, *103*, 653.
(32) Czandema, A. W.; King, D. E.; Spauling, D. *J. Vac. Sci. Technol. A* **1995**, *9*−*5*, 2607.
(33) Vogt, A. D.; Han, T.; Beebe, T. B., Jr. *Langmuir* **1997**, *13*, 3397.
(34) Wagner, C. D.; Naumkin, A. V.; Kraut-Vass, A.; Allison, J. W.; Powell, C. J.; Rumble, J. R., Jr. NIST X-ray Photoelectron Spectroscopy Database 20, Version 3.4, Standard reference data program of the National Institute of Standards and Technology; NIST: Gaithersburg, MD, 2003.
(35) Beamson, G.; Briggs, D. *High-Resolution XPS of Organic Polymers − The Scienta ESCA Database*; John Wiley & Sons Ltd.: Chichester, U.K., 1992.
(36) Fustin, C. A.; Gouttebaron, R.; De Nadaï, C.; Caudano, R.; Zerbetto, F.; Leigh, D. A.; Rudolf, P. *Surf. Sci.* **2001**, *474*, 37.
(37) Whelan, C. M.; Cecchet, F.; Clarkson, G. J.; Leigh, D. A.; Caudano, R.; Rudolf, P. *Surf. Sci.* **2001**, *474*, 71.
(38) From Origin6.0, Microcal Software Inc., Nothampton, MA.
(39) Bureau, Ch. Private communication.
(40) O'Shea, J. N.; Schnadt, J.; Brühwiler, P. A.; Hillesheimer, H.; Mårtensson, N. *J. Phys. Chem. B* **2001**, *105*, 1917.
(41) Arnold, R.; Azzam, W.; Terfort, A.; Wöll, C. *Langmuir* **2002**, *18*, 3980.
(42) Wirde, M.; Gelius, U.; Dunbar, T.; Allara, D. L. *Nucl. Instrum. Methods Phys. Res. B* **1997**, *131*, 245.
(43) Heister, K.; Zharnikov, M.; Grunze, M.; Johansson, L. S. O.; Ulman, A. *Langmuir* **2001**, *17*, 8.
(44) Zharnikov, M.; Frey, S.; Heister, K.; Grunze, M. *Langmuir* **2000**, *16*, 2697.
(45) Mekhalif, Z.; Riga, J.; Pireaux, J.-J.; Delhalle, J. *Langmuir* **1997**, *13*, 2285.
(46) Finklea, H. O. In *Electroanalytical Chemistry*; Bard, A. J., Ed.; Marcel Dekker: New York, 1996; Vol. 19, p 109.
(47) Flink, S.; van Veggel, F. C. J. M.; Reinhoudt, D. N. *Adv. Mater.* **2000**, *12*, 1315.
(48) MacDonald, J. R. *Impedance Spectroscopy; Emphasizing Solid Materials and Systems*; Wiley: New York, 1987.
(49) Bard, A. J.; Faulkner, L. R. *Electrochemical Methods*, 2nd ed.; Wiley: New York, 2001.
(50) Amatore, C.; Saveant, J. M.; Tessier, D. *J. Electroanal. Chem.* **1983**, *147*, 39.
(51) Becka, A. M.; Miller, C. *J. Phys. Chem.* **1992**, *96*, 2657.
(52) Terrettaz, S.; Becka, A. M.; Miller, C. *J. Phys. Chem.* **1995**, *99*, 11216.
(53) Gafni, Y.; Weizman, H.; Libman, J.; Shanzer, A.; Rubinstein, I. *Chem. Eur. J.* **1996**, *2*, 759.
(54) Rubinstein, I.; Sabatani, E.; Rishpon, J. *J. Electrochem. Soc.* **1987**, *134*, 3078.
(55) Boukamp, B. A. *Solid State Ionics* **1986**, *20*, 31.
(56) (a) Protsailo, L. V.; Fawcett, W. R. *Electrochim. Acta* **2000**, *45*, 3497. (b) Dijksma, M.; Boukamp, B. A.; Kamp, B.; van Bennekom, W. P. *Langmuir* **2002**, *18*, 3105. (c) Cui, X.; Jiang, D.; Diao, P.; Li, J., Tong, R.; Wang, X. *J. Electroanal. Chem.* **1999**, *470*, 9. (d) Janek, R. P.; Fawcett, W. R.; Ulman, A. *J. Phys. Chem. B* **1997**, *101*, 8550.
(57) Finklea, H. O.; Avery, S.; Lynch, M.; Furtsch, T. *Langmuir* **1987**, *3*, 409.
(58) Diao, P.; Jiang, D.; Cui, X.; Gu, R.; Tong, D.; Zhong, B. *J. Electroanal. Chem.* **1999**, *464*, 61.
(59) Miller, C.; Cuendet, P.; Grätzel, M. *J. Phys. Chem.* **1991**, *95*, 877.
(60) Colton, R. J., Engel, A., Frommer, J. E., Gaub, H. E., Gewirth, A., Guckenberger, R., Heckl, W. M., Parkinson, B., Rabe, J., Eds. *Procedures in Scanning Probe Microscopies*; John Wiley & Sons Ltd.: New York, 1998.
(61) Barros, T. C.; Berci, P.; Toscano, V. G.; Politi, M. J. *J. Photochem. Photobiol. A: Chem.* **1995**, *89*, 141.
(62) Barros, T. C. *J. Photochem. Photobiol. A: Chem.* **1993**, *76*, 55.